Solvent-Dependent Photoacidity State of Pyranine Monitored by Transient Mid-Infrared Spectroscopy

Omar F. Mohammed,[a] Jens Dreyer,[a] Ben-Zion Magnes,[b] Ehud Pines,[b] and Erik T. J. Nibbering*[a]

We investigate with femtosecond mid-infrared spectroscopy the vibrational-mode characteristics of the electronic states involved in the excited-state dynamics of pyranine (HPTS) that ultimately lead to efficient proton (deuteron) transfer in H_2O (D_2O). We also study the methoxy derivative of pyranine (MPTS), which is similar in electronic structure but does not have the photoacidity property. We compare the observed vibrational band patterns of MPTS and HPTS after electronic excitation in the solvents: deuterated dimethylsulfoxide, deuterated methanol and H_2O/D_2O, from which we conclude that for MPTS and HPTS photoacids the first excited singlet state appears to have charge-transfer (CT) properties in water within our time resolution (150 fs), whereas in aprotic dimethylsulfoxide the photoacid appears to be in a nonpolar electronic excited state, and in methanol (less polar and less acidic than water) the behaviour is intermediate between these two extremes. For the fingerprint vibrations we do not observe dynamics on a time scale of a few picoseconds, and with our results obtained on the O–H stretching vibration we argue that the dynamic behaviour observed in previous UV/Vis pump–probe studies is likely to be related to solvation dynamics.

1. Introduction

Photoacidity, the property of light-absorbing molecules that are more acidic in the excited electronic state than in the ground state, has been a long standing subject of research.[1–10] Photoacids are known to donate a proton in aqueous solutions, or even in less polar solvents in the case of enhanced photoacids, where electron-withdrawing groups, such as cyano, sulfonate or perfluoroalkylsulfonyl groups, have been introduced.[7] The mechanism of the excited-state proton transfer (ESPT) to water, which typically occurs with relatively slow pace on time scales of tens to hundreds of picoseconds,[6] remains unclear. Several models for the molecular origins of photoacidity have been proposed in which either the optically accessible excited state is directly responsible for the photoacidity [two-state charge-transfer (CT) model; Figure 1a] or level crossing to electronic states with different degrees of acidity are involved [three-state locally excited charge-transfer (LE-CT) model, Figure 1b, and three-state excited-state hydrogen-transfer ESHT model, Figure 1c].

Traditionally the nature of the acidity of the photoacid S_1 state has been ascribed to intramolecular charge transfer from the nonbonding orbital of the hydroxyl oxygen to the aromatic ring π^* orbital.[11–15] The Coulombic repulsion between the partial positive charge on the O atom and the H atom is then considered to lead to the enhanced acidity in the S_1 state. In this picture the excited state proton transfer dynamics, controlled by barrier crossing, is described by a two-state model (Figure 1a), where an optically excited photoacid state converts into an excited conjugated photobase upon proton transfer.[16–26]

A second model invokes the occurrence of and the internal conversion between nearby lying electronic excited levels of the photoacid (Figure 1b). Typically two spectroscopically accessible states can be reached for aromatic molecules upon electronic excitation, either with light polarized along the through-bond axis (^1L_b state) or along the through-atom axis

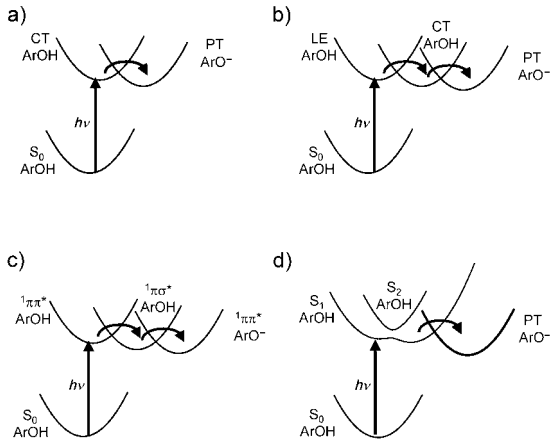

Figure 1. *Different models used to explain the excited state reaction dynamics of photoacids: two-state model (a); the three-state model with nonadiabatic crossing between the LE(^1L_b) and CT(^1L_a) states (b); the excited-state hydrogen transfer model with $^1\pi\pi^*$ and $^1\pi\sigma^*$ levls involved (c); and the strongly coupled adiabatic evolution between strongly mixed ^1L_b and ^1L_a states (d).*

[a] *O. F. Mohammed, Dr. J. Dreyer, Dr. E. T. J. Nibbering*
Max Born Institut für Nichtlineare Optik und Kurzzeitspektroskopie
Max Born Strasse 2A, 12489 Berlin (Germany)
Fax: (+49) 30-6392-1409
E-mail: nibberin@mbi-berlin.de

[b] *Dr. B.-Z. Magnes, Prof. Dr. E. Pines*
Department of Chemistry, Ben-Gurion University of the Negev
P.O.B. 653, Beer-Sheva 84125 (Israel)

 DOI: 10.1002/cphc.200400510

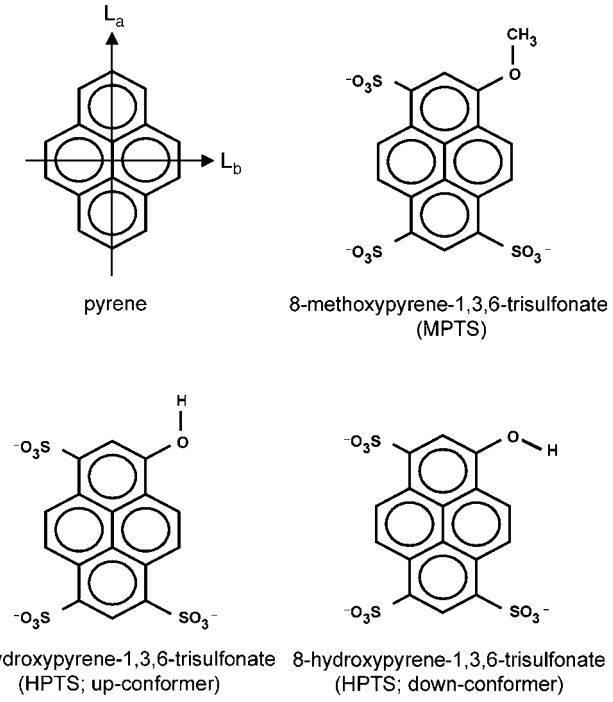

Figure 2. *Molecular structures for MPTS and HPTS (shown in the up- and down-conformations). The direction of excitation to ^1L_b and ^1L_a states in the case of naphthalene are also indicated.*

(^1L_a state), see also Figure 2. For aromatic molecular systems such as indoles,[27–33] tryptophane,[34] or pyrene derivatives[35] internal conversion between these ^1L_b and ^1L_a levels has been suggested in the interpretations. For 1-naphthol[36,37] the $^1L_b \rightarrow {}^1L_a$ transition is considered to be the ESPT-determining step[9,38,39] In contrast, in a recent combined experimental/theoretical study of ESPT of pyranine[40–42] the rate determining step is not the conversion from the optically accessible locally excited (LE) state (or alternatively the ^1L_b state), to the second photoacid electronic excited n–π^* CT state (or ^1L_a state), but the transition of the photoacid CT to photobase CT states.

A third model, where rather excited state hydrogen transfer (ESHT) is supposed to occur[43,44] (Figure 1 c), has recently emerged from excited-state dynamics studies of gas-phase phenol clustered with ammonia or water molecules.[10] In this model it is argued that due to a level crossing between the initially excited $^1\pi\pi^*$ state and a $^1\pi\sigma^*$ state a migration of an electron occurs from the photoacid to the solvent, followed by the proton of the hydroxyl group, with a net transfer of a hydrogen atom as a result. Modelling photoacidity as ESHT has also been used to explain an experiment where donor and acceptor groups are connected through a wire of ammonia molecules.[45] A conical intersection of the $^1\pi\sigma^*$ state with the S_0 state leads to an efficient internal conversion pathway for phenol–ammonia clusters. Net proton transfer on the other hand should involve at least one more step with an electron back-transfer to the photoacid, producing the photobase and solvated proton as separate species.

Herein, we investigate the excited state photoacidic properties of pyranine (8-hydroxy-1,3,6-trisulfonate pyrene; HPTS) in liquid solution (see Figure 2). In Figure 3, the electronic absorption and emission spectra of HPTS are shown for the solvents dimethylsulfoxide, methanol and water. In particular for water,

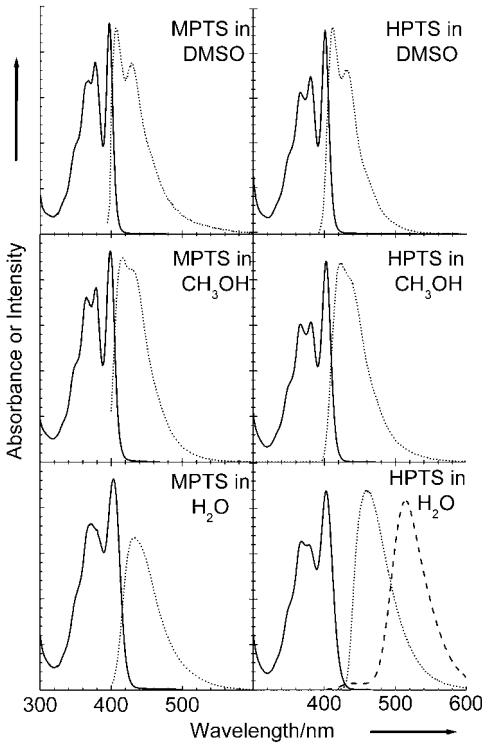

Figure 3. *Electronic absorption and emission spectra of HPTS and MPTS in dimethylsulfoxide, methanol and water.*

mirror symmetry between the absorption and emission bands of HPTS is absent, hinting at strong rearrangements in the excited state. A solvatochromic study of HPTS in a variety of solvents has been performed where the absorption and emission frequency shifts were interpreted assuming excitation and emission from a single electronic state.[46] In another study of solvatochromic properties of absorption and emission bands of HPTS[41] and the time-resolved UV-pump/Vis-probe study[40] by Thran-Thi et al., the conclusion has been drawn that the observed features can be explained by the three-state LE-CT model, with the LE(^1L_b)→CT(^1L_a) state inversion taking place with a time constant of about 2 ps. Our approach is to characterise the nature of the excited electronic states by inspection of the associated infrared-active vibrations with time-resolved spectroscopy. We present results obtained with femtosecond mid-infrared spectroscopy on HPTS dissolved in water, deuterated water, deuterated methanol (CD_3OD; MeOD) and deuterated dimethylsulfoxide ([D_6]DMSO). These solvents have been chosen since a) [D_6]DMSO is only a hydrogen acceptor, whereas MeOD and H_2O/D_2O are both hydrogen aceptors and donors; b) proton–deuteron transfer only occurs in H_2O/D_2O and not in MeOD. We thus explore not only the level structure of the singlet excited states but also the intricacies related to

hydrogen bonding. We excite HPTS either close to the electronic origin around 400 nm or with vibrational excess energy at 350 nm. From this we estimate the importance of possible contributions of the LE(^1L_b) and CT(^1L_a) states to the observed electronic absorption bands and related dynamics. We report the transient infrared bands of the photoacid, and their associated dynamics under the different excitation conditions. For comparison we also investigate the dynamics of 8-methoxy-1,3,6-trisulfonate pyrene (MPTS) in the same solvents (Figures 2 and 3). MPTS is very similar to HPTS from an electronic structural point of view (same level structure and similar energetics). In addition, possible hydrogen-bonding dynamics are expected to be similar at the sulfonate side groups. However, the difference between MPTS and HPTS lies in the photoacidity property only present for the latter compound. From this comparison we can derive possible contributions to the observed transients by hydrogen-bonding dynamics at either the sulfonate or the hydroxyl groups.

Experimental Section

In the femtosecond mid-infrared experiments we used 15–20 mM solutions of HPTS (pyranine, or 8-hydroxy-1,3,6-trisulfonate pyrene, Aldrich) or of MPTS (8-methoxy-1,3,6-trisulfonate pyrene; Fluka) in D_2O, CD_3OD, $(CD_3)_2SO$ (Deutero, 99.8% deuteration grade) when exciting in the electronic origin at 400 nm. We used a concentration of 30–40 mM when exciting in the wing of the electronic band at 350 nm. We excited a 100 μm thick jet or a home-built rotating sample cell consisting of 1 mm thick CaF_2 windows with a 100 μm thick teflon spacer containing the sample solutions with the second harmonic of a home built 1 kHz amplified Ti:sapphire laser system (wavelength 400 nm, pulse duration 55 fs, energy 3–7 μJ, spot diameter 200 μm) or with pulses centred at 350 nm (pulse duration 50 fs, energy 1–3 μJ, same spot diameter) generated by sum-frequency mixing of the fundamental with visible pulses obtained with a noncollinear parametric amplifier.[47] Tunable mid-infrared probe pulses of 100–150 fs duration were generated by difference frequency mixing of signal and idler pulses from a near-infrared optical parametric amplifier.[48] After spectral dispersion with a polychromator the probe pulses were detected by a multichannel detector for the mid-IR. The whole pump–probe setup was purged with nitrogen gas to avoid spectral and temporal reshaping of the mid-IR pulse by the absorption of water vapour in the air. The time resolution was determined to be 120–140 fs based on cross-correlation measurements between UV-pump/IR-probe pulses and on estimations of group velocity mismatch between the UV and IR pulses. At intense excitation conditions often a strong transient absorbance signal due to multiphoton absorption effects was observed, decaying with a time constant of about 300 fs. Since this multiphoton-induced signal appears to be frequency-independent, effectively leading to a floating baseline, we were in this case also able to detect the narrow spectral features of the transient infrared-active vibrations as early as 100–150 fs.

In order to interpret the experimental results, we performed theoretical calculations of vibrational spectra at optimised structures for HPTS (in photoacid and in conjugated photobase forms) and for MPTS. We applied density functional theory [B3LYP/6-31+G(d,p)] methods as implemented in Gaussian 98.[49]

2. Experimental Results

2.1 Ground-State Vibrational Spectra of MPTS and HPTS Photoacids and Photobases

In Figures 4 and 5 we compare the experimental IR spectra of MPTS and of HPTS in H_2O/D_2O with the calculated ground-

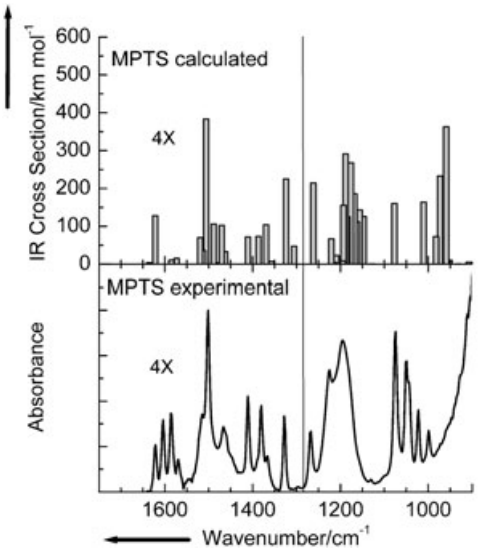

Figure 4. Comparison of the calculated and experimental fingerprint IR-active bands of MPTS in the electronic ground state. The spectral range of 900–1280 cm^{-1} was measured in H_2O, and 1250–1750 cm^{-1} in D_2O. The experimental and theoretical band intensities in the frequency range of 1280–1750 cm^{-1} have been expanded by a factor of four.

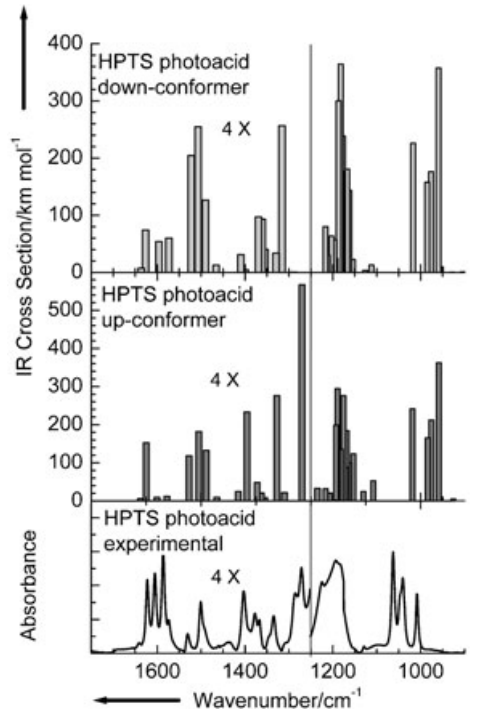

Figure 5. Comparison of the calculated and experimental fingerprint IR-active bands of the HPTS photoacid in the electronic ground state. The spectral range of 900–1280 cm^{-1} was measured in H_2O, and 1250–1750 cm^{-1} in D_2O. The experimental and theoretical band intensities in the frequency range of 1280–1750 cm^{-1} have been expanded by a factor of four.

state spectra (see also Table 1). Note that the calculated IR band pattern shows marked intensity variations depending on the HPTS conformer as given by the relative orientation of the hydroxy group with respect to the aromatic ring. The calculations indicate a small energy difference between the two conformers of about 75 cm^{-1}, with the up-conformer being the more stable one. The relative stability of the two conformers will probably be solvent dependent, but we expect that both conformers will be present in significant amounts in all solvents used in the experiments. In addition we show the IR spectra for the conjugate photobase of HPTS in Figure 6, that has been measured in a solution of HPTS in 0.02 M NaOH. From the calculations we learn that the following grouping of bands in the fingerprint region can be made. The vibrational transitions of modes involved in motions of the sulfonate groups are found between 950–1100 cm^{-1} (Ar–SO_3^- stretching modes) and between 1100–1250 cm^{-1} (S–O stretching modes). These modes do not change their characteristics significantly when the HPTS photoacid converts into the conjugate photobase. Modes predominantly involving aromatic ring deformations, and modes where the C–O stretching and aromatic ring deformation vibrations participate are found in the range of 1250–1650 cm^{-1}. From the calculations we learn that no isolated C–O stretching vibration occurs for the HPTS photoacid, and the same applies for the photobase. However, since a transition from photoacid to photobase due to proton transfer is accompanied by a change in the electronic charge distribution, the vibrational transitions due to modes with C–O stretching content will change in the frequency position and absorption cross-section.[50,51] This is most pronounced when comparing the IR spectra of the ground-state HPTS photoacid and photobase in the frequency range between 1450–1600 cm^{-1}.

Despite a rescaling of the calculated frequencies an entirely satisfying correspondence between experiment and theory cannot be reached for all transitions. The reason for that lies in the frequency changes induced by hydrogen bonding, where vibrational motions involving either the sulfonate or the hydroxy groups will be affected when a hydrogen bond is formed with the solvent, whereas vibrational modes that comprise aromatic ring nuclear motions only are expected to remain relatively unchanged.

Table 1. *Calculated frequencies of the infrared-active fingerprint vibrations of HPTS and MPTS in the photoacid (two conformers) and photobase forms.*

Assignment[a]	HPTS photoacid up-form[b]	HPTS photoacid down-form[c]	HPTS photobase[d]	MPTS up-form[e]
γCH			969	
δS–O + δpyr	978	979	970[f]	978
δS–O + νC–S + νC–O + δpyr	996, 1004	996, 1005	992, 1000	993, 1002
νC–S + δpyr + νC–O	1039	1038	1037	1031
δpyr + νH_3C–O + νC–S				1099, 1170
δpyr + δCH + δOH	1131	1135		
δpyr + δCH	1153	1149	1130	1151
νS–O(ip) + δCH + δOH and νS–O(oop) + γCH	1177–1217	1178–1221	1168–1186	1180–1218
δCH + δOH + νS–O	1232	1228		1234
δCH + δOH	1260			
δCH + δpyr + δOH νC–O + δCH + δOH	1241 1296	1237, 1242 1318[f]	1203–1235	1246 1287
νpyr + δCH + δOH + νC–O	1355, 1337[f]	1357, 1343, 1397		1351, 1397
νpyr + δCH + δOH	1424	1438	1290–1456	1332, 1415, 1440
δCH_3				1501
δCH_3 + νpyr				1493, 1519, 1537, 1544
νpyr	1519, 1536	1521, 1538	1510, 1522	
νpyr + δOH/δCH_3	1559, 1658	1554, 1629, 1660, 1605		1559
νpyr + νC–O			1481, 1563–1646	1605, 1618, 1655

[a] δ = in-plane (ip) deformation, γ = out-of-plane (oop) deformation, ν = stretching, pyr = pyrene. [b] E = −2560.59484 a.u. [c] E = −2560.59450 a.u. (ΔE = +75 cm^{-1}), OH twisted oop by 17°. [d] E = −2559.79529 a.u. (no δOH contributions). [e] E = −2599.89993 a.u. (no δOH contributions). [f] Weak band.

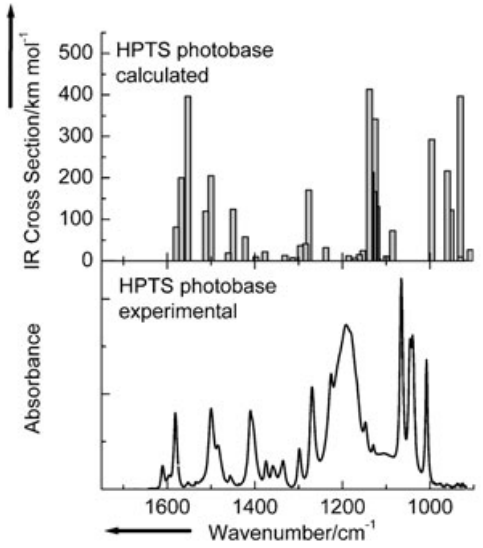

Figure 6. *Comparison of the calculated and experimental fingerprint IR-active bands of the HPTS conjugated photobase in the electronic ground state. The spectral range of 900–1280 cm^{-1} was measured in H_2O, and 1250–1750 cm^{-1} in D_2O.*

This is clear when one inspects the experimental IR spectra of MPTS and of the HPTS photoacids in the solvents [D_6]DMSO, MeOD and D_2O in the range of 1250–1700 cm^{-1} (see Figure 7). The vibrational transitions of MPTS only show minor solvent shifts of at most 2–3 cm^{-1}. Since only the vibrational modes of MPTS involving the sulfonate groups will be affected by hydrogen bonding (with hydrogen donors such as methanol or water), only these bands may have substantial solvent shifts. The vibrational modes of the aromatic ring and/or methoxy side group in MPTS will not change their characteristics due to hydrogen bonding. This is different for HPTS, where besides several vibrational bands of the sulfonate side groups also vibrational transitions, where the hydroxy group is involved show substantial influence of the solvents used. In the case of the HPTS photoacid the hydroxy group will form a hydrogen bond with the hydrogen acceptor dimethylsulfoxide and in the case of methanol and water either by hydrogen donating or accepting with solvent molecules. For the HPTS photoacid thus larger solvent-induced frequency shifts (as well as absorbance changes) occur in the frequency range of 1250–1700 cm^{-1}, depending on the hydrogen-bonding capability of the solvent. Care must thus be taken when interpreting solvent-induced frequency shifts and band strengths in the time-resolved experiments presented in the next section.

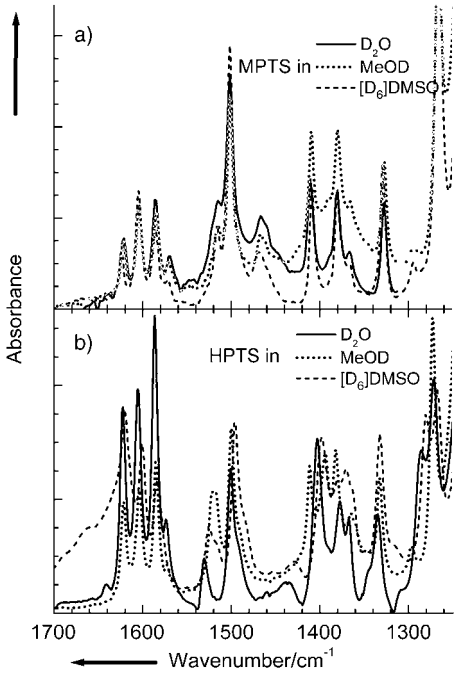

Figure 7. *Comparison of the experimental IR spectra of MPTS (a) and HPTS photoacid (b) in the three solvents [D_6]DMSO, MeOD and D_2O.*

2.2 Transient Vibrational Dynamics of MPTS and HPTS Photoacids after Electronic Excitation

We have investigated the response in the O–H stretching region for HPTS in DMSO and in H_2O (Figures 8–11). In the case of DMSO we have observed a transient absorption band be-

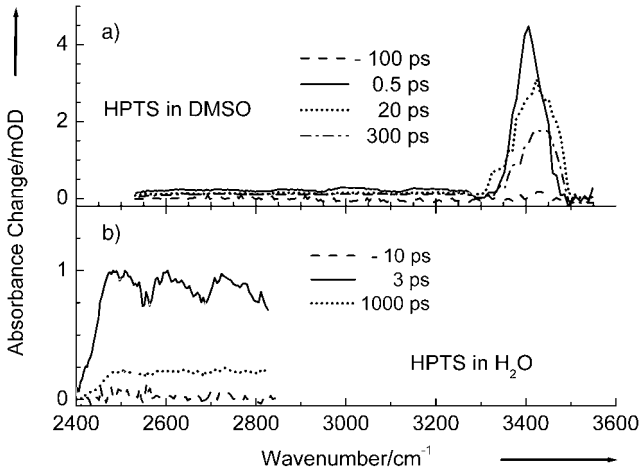

Figure 8. *Transient spectra of O–H stretching band of HPTS in DMSO/[D_6]DMSO (a) and in H_2O (b) after excitation at 400 nm.*

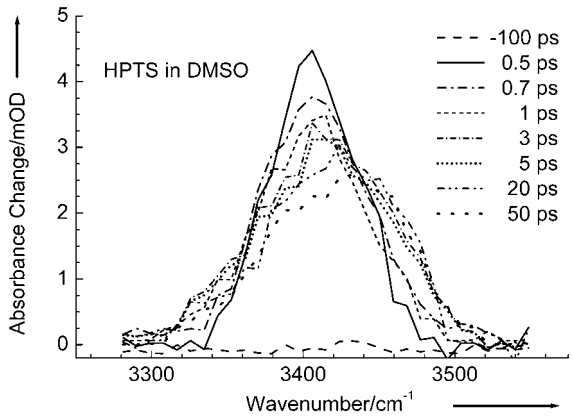

Figure 9. *Transient spectra of O–H stretching band of HPTS in DMSO after excitation at 400 nm showing the decrease in magnitude and small frequency upshift for longer pulse delays.*

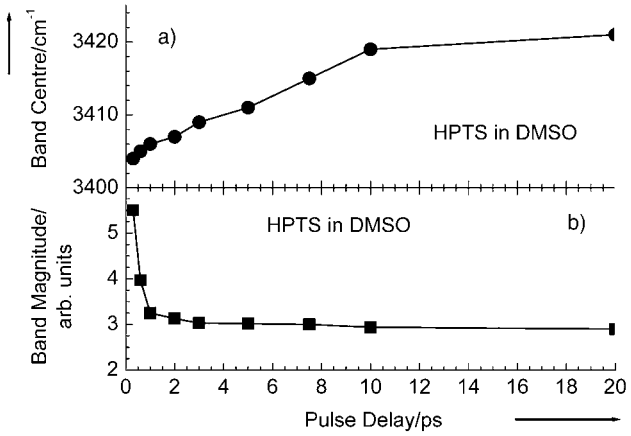

Figure 10. *Band centre and band magnitude of the O–H stretching band of HPTS in DMSO after excitation at 400 nm as function of the pulse delay.*

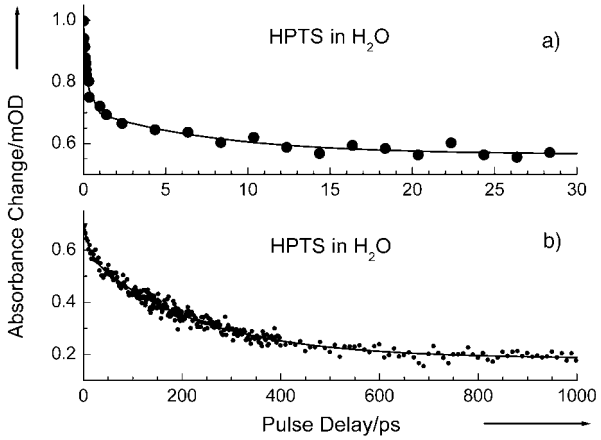

Figure 11. *Magnitude of the transient O–H stretching response of HPTS in H_2O after excitation at 400 nm as function of the pulse delay, showing the influence of solvation dynamics at short times (a) and proton transfer and rotational diffusion at longer times (b).*

tween 3300 and 3500 cm^{-1}, that appears within time resolution. We assign this transient band to the O–H stretching band of HPTS in the excited state. This absorption must be overlapping with the O–H stretching band in the ground state in frequency position. The absorption cross-section of the O–H stretching band in the electronic excited state must be significantly larger than that in the ground state, as we do not observe bleaching contributions in the transient response that can be associated with the disappearance of ground state population. The transient band rearranges in shape, frequency position, and magnitude, with temporal components of 300 ± 200 fs, 4 ± 2 ps and 150 ± 50 ps (Figures 9 and 10). For HPTS in H_2O we cannot probe the opaque frequency region between 2850 and 3700 cm^{-1}, where one would expect the O–H stretching band of HPTS in the ground and excited states. However, for frequencies below 2850 cm^{-1} we have detected a transient absorbance, that decays in multiexponential fashion with 300 ± 200 fs and 3.0 ± 1.5 ps time components at short pulse delay (Figure 11), and long time behaviour that we can fit with 90 ± 30 and 200 ± 50 ps components. The cut-off around 2400 cm^{-1} is due to a bandpass filter we used to suppress unwanted idler light in the direction of our detector.

In Figure 12 we show the transient absorbance changes of MPTS and HPTS in the fingerprint region in the three solvents [D_6]DMSO, MeOD and D_2O 300 fs after electronic excitation.

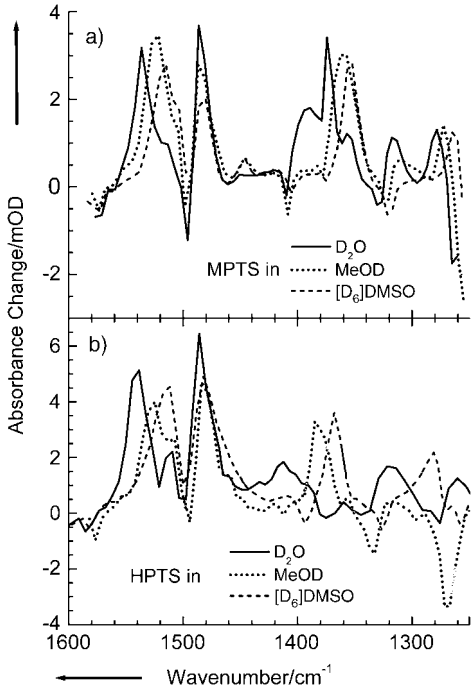

Figure 12. *Transient IR absorbance changes after excitation at 400 nm recorded at a 300-fs pulse delay of MPTS and HPTS dissolved in the three solvents [D_6]DMSO, MeOD and D_2O.*

These changes appear within our time resolution of 150 fs. Negative contributions indicate bleach signals located at frequencies of vibrational transitions of MPTS and HPTS in the electronic ground state. Positive contributions are indicative of vibrational transitions of MPTS/HPTS in the electronic excited state reached within our time resolution. Typically for MPTS and HPTS positive signals indicating vibrational transitions of the electronic excited state are stronger than the bleach signals due to ground state vibrational bands. Within the first tens of picoseconds no additional dynamics of the vibrational bands of MPTS/HPTS in the electronic excited state are observed.

The transient spectra show a solvent dependence for both MPTS and HPTS (see Figure 12). Marked differences between these transient spectra can be noted. In the case of MPTS and HPTS the spectra obtained for [D_6]DMSO clearly deviate from those for D_2O, with the case MeOD somewhere in between. In particular, MPTS shows a broad band at 1353 cm^{-1} in [D_6]DMSO and MeOD, whereas in D_2O a narrow band only is present at 1375 cm^{-1}. A band at 1452 cm^{-1} is present in [D_6]DMSO and MeOD, whereas this band appears to be absent in D_2O. On the other hand a vibrational transition at 1318 cm^{-1} is clearly visible in the spectrum obtained with D_2O, which is

smaller in magnitude in MeOD, and fully absent in [D_6]DMSO. A band at 1516 cm^{-1} is observed in [D_6]DMSO, in MeOD it is upshifted to 1522 cm^{-1},and in D_2O it appears at 1536 cm^{-1}. A strong IR-active transition at 1488 cm^{-1} appears in all solvents.

A similar solvent-dependent variation of the vibrational pattern is observed in the same part of the fingerprint region for HPTS. A band at 1288 cm^{-1} is only present in [D_6]DMSO, a transition at 1380 cm^{-1} is observed in [D_6]DMSO and MeOD and not in D_2O, bands at 1314 and 1415 cm^{-1} appear only in D_2O. A relatively strong IR-active transition at 1518 cm^{-1} in [D_6]DMSO appears to be shifted to 1525 cm^{-1} in MeOD and to 1546 cm^{-1} in D_2O, revealing another transition at 1517 cm^{-1}. Again a band at 1488 cm^{-1} is present in all solvents.

In the case of [D_6]DMSO and MeOD there is no evidence for proton/deuteron transfer occuring within the electronic excited state lifetime of HPTS. This is in accord with HPTS being a much weaker acid when in the electronic ground state, and consequently also in the excited state in these solvents than in the case of water. Any changes in signal strengths occuring on longer time scales are the consequence of rotational diffusion. The same applies for the recorded signals for MPTS in all three solvents, where proton transfer is not possible. In contrast, for HPTS proton (deuteron) transfer takes place with a time constant of about 90 ps (250 ps) in H_2O (D_2O). As a result, the transient bands of the HPTS photoacid change their magnitude not only because of rotational diffusion, but also because it converts into the conjugate photobase, as indicated by an ingrowth of photobase bands. We have reported in a previous acid–base neutralization study[50] how changes of the transient spectrum of HPTS in the range around 1500 cm^{-1}, where the strongest bands of the excited state photoacid and photobase species occur for the upper half of the fingerprint region, indicate the transition from the photoacid to the photobase, when a deuteron transfer to an accepting base takes place.

The transient spectra of HPTS in [D_6]DMSO or D_2O after excitation at 350 nm recorded in the same range show basically the solvent-dependent appearance of the same IR-active bands within time resolution (Figure 13). The bands however appear slightly red-shifted with a larger initial bandwidth. With a time constant of 5–10 ps these bands blue-shift to the same frequency position as observed when exciting HPTS in [D_6]DMSO or D_2O at 400 nm, accompanied by a slight narrowing. From pulse delays of 20 ps onwards the dynamics of these bands are identical for both excitation wavelengths.

3. Discussion

3.1. Solvent-Dependent Vibrational-Mode Patterns of MPTS and HPTS

Our results obtained on the response of the O–H stretching vibration of HPTS in DMSO and in H_2O (Figures 8–11) reveal two important properties of the excited states of HPTS. It is well known that the IR-active band of the O–H stretching oscillator provides a direct probe of the strength of the hydrogen bond.[52,53] The larger the red-shift, accompanied by larger broadening and larger cross-section, the stronger the hydrogen bond of the O–H group with hydrogen acceptors. In the case of HPTS in the excited state dissolved in DMSO we observe an O–H stretching band that appears around 3400 cm^{-1}, typical for weak hydrogen bonds such as those in water, and alcohols. We are able to observe this band only because of higher IR cross-sections for the O–H stretching vibration in the electronic excited than in the ground state of HPTS. This may hint at an increase of hydrogen bond interaction of the photoacid upon electronic excitation. Interpretation of electronic-state-dependent changes in vibrational cross-sections, however, have to be taken with care, as shown in a recent study of hydrogen-bond interactions of a coumarin dye with phenol molecules affected by electronic excitation of the coumarin chromophore.[54] After appearance of the transient O–H stretching band we observe a broadening and slight upshifting of this band with 300 ± 200 fs and 4 ± 2 ps time constants. This observation indicates a rearrangement of the hydrogen bond of HPTS with the solvent DMSO molecules, that we ascribe to solvation dynamics that is also expected to occur on these time scales. The change in magnitude of the transient O–H band with the long time component of 150 ± 50 ps is caused by rotational diffusion of HPTS.

In contrast, although we cannot probe the 2850–3700 cm^{-1} region because of absorbance of the solvent H_2O, we do observe a transient response of HPTS in H_2O at even lower frequencies. We can assign the observed transient signal between 2400–2800 cm^{-1} to the O–H stretching frequency of HPTS in the photoacid state because: a) no signal was observed in H_2O only (excluding transient absorption by species generated by multiphoton absorption), and b) no signal was observed for the case of MPTS. In particular the latter observation means that no transient response of water molecules attached to the sulfonate groups contributes in this frequency range. Instead these water molecules form weak hydrogen bonds with the sulfonate groups, having their response in the range of bulk water around 3400 cm^{-1}. In addition we can exclude a transient response of "hot" water molecules in the first solvation shell that would be generated after vibrational energy dissipation from HPTS to the solvent. The reason for this is that "hot" water molecules would exhibit a blue-shifted O–H stretching response (as a consequence of a weakened hydrogen bond in these "hot" molecules),[53] and a *decrease* of transient absorbance would result in the low-frequency wing of the O–H stretching band of water. In contrast we observe an *increase* of transient response within time resolution and, thus, this signal indicates the O–H stretching transition of HPTS in the electronic excited state. This implies a significant enhancement of the hydrogen bond strength of the O–H group of HPTS in H_2O compared to HPTS in DMSO, resulting in the occurrence of medium-strong hydrogen bonds with more red-shifted O–H stretching absorption.[52] This points at a change in electronic structure of HPTS in water compared to the situation of HPTS in DMSO. A mechanistic view of such a solvent mediated level structure of HPTS has been considered by Tran-Thi et al..[40,41] In this model a stronger acidity is expected in the CT(^1L_a) state of HPTS compared to photoacidity of the LE(^1L_b) state, and a stronger hydrogen bond is consistent with this picture.

The magnitude of the response of the O–H stretching oscillator of HPTS in H_2O is observed to decay in a multiexponential fashion. We ascribe again the 300 ± 200 fs and 3.0 ± 1.5 ps components to solvent rearrangements affecting the hydrogen bond of HPTS with nearby H_2O molecules. The decaying behaviour at long pulse delays with 90 ± 30 and 200 ± 50 ps time components are caused by the proton transfer to the solvent and rotational diffusion. A small remaining signal at even longer pulse delays might be due to the O–H stretching oscillators of water molecules hydrogen bonded to the HPTS conjugated photobase species.

In contrast, we do not observe any changes in frequency position of the vibrational patterns in the fingerprint region for MPTS and HPTS in the electronic excited state in all solvents investigated from 150 fs (our time resolution) up to 20 ps (Figure 12). Only at longer time scales the band intensities of MPTS and HPTS are affected by rotational diffusion. In addition, the case of HPTS proton (deuteron) transfer takes place in H_2O (D_2O) with a 90 (250) ps time constant. These observations teach us that MPTS and HPTS do not change their electronic state in the time range from 150 fs–20 ps, and accordingly the changes observed in the O–H stretching region must be due to solvation dynamics. However, the vibrational band patterns in [D_6]DMSO are clearly distinct from those observed in D_2O, with the cases of MeOD somewhat intermediate between these two.

From the steady-state IR spectral analysis of MPTS and HPTS in the electronic ground state we derive that the fingerprint vibrations of MPTS in the frequency range of 1250–1750 cm^{-1} are not affected by the hydrogen-donating and accepting capability of the solvents used. Rephrasing this statement: MPTS hydrogen bonds can only be formed with its sulfonate groups, whose vibrational bands can be found in the range of 850–1250 cm^{-1}. In contrast, HPTS hydrogen bonds can be formed with its sulfonate and its hydroxyl functionality. Here, spectral changes in the full fingerprint region may be caused by altered hydrogen-bonding interactions.

The excited-state vibrational patterns are both for MPTS and HPTS dependent on the solvent used. Since we can use the same argument for MPTS in the electronic excited state that hydrogen bonds do not affect the vibrational transitions in the higher frequency part of the fingerprint region, we can conclude that the different transient IR spectra observed in the solvents [D_6]DMSO, MeOD and D_2O are the consequence of different charge distributions in the excited state of MPTS. The femtosecond mid-infrared transient spectra thus reveal the occurrence of a solvent-dependent electronic state change when going from [D_6]DMSO, via MeOD to D_2O. By similarity we conclude that the same argument applies for HPTS, although here hydrogen bonding with the hydroxyl group will have an influence on frequency shifts of the observed IR-active vibrations as well.

Summarizing this section, we conclude that both the O–H stretching region of HPTS and the fingerprint regions of HPTS and MPTS reveal the occurrence of a solvent-affected electronic excited-state structure of HPTS and MPTS.

3.2. Excitation with Vibrational Excess Energies

An additional question that may be tackled in the photodynamics of HPTS is whether the absorption band between 320–430 nm is due to one electronic transition, or as suggested by the three state models it is the result of two electronic transitions with absorption cross-sections of similar magnitudes. When exciting at 350 nm, an excess energy of 3650 cm^{-1} is put into the HPTS photoacid relative to the electronic origin transition of the (LE–^1L_b, or $^1\pi\pi^*$) state around 405 nm. In the case that the same electronic state is reached with excitation at 350 nm this excess energy is initially located in the totally symmetric Raman-active modes that show strong Franck–Condon activity upon electronic excitation. On the other hand, if the second (CT-^1L_a, or $^1\pi\sigma^*$) state is reached the vibrational excess energy in Raman-active modes may initially be less or more, depending on the exact location of the the origin transition of the (CT-^1L_a, or $^1\pi\sigma^*$) state.

As indicated in Figure 13 we observe IR-active vibrations that appear red-shifted because of anharmonic coupling with

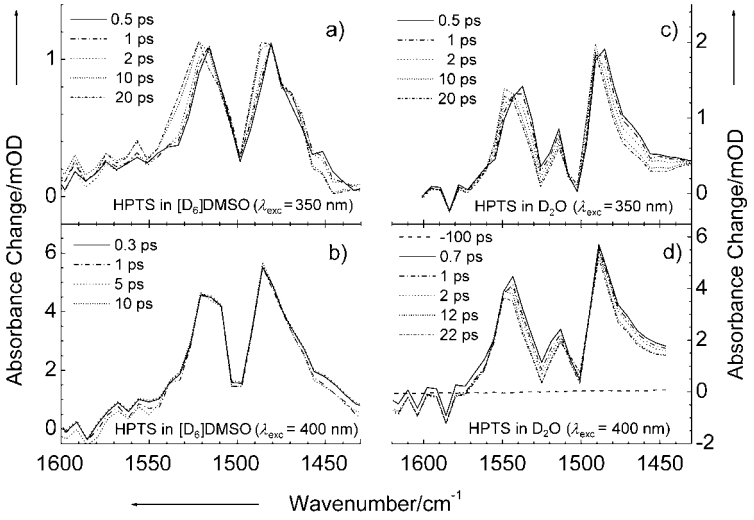

Figure 13. *Comparison of the transient IR absorbance changes after excitation at 350 nm (a,c) and at 400 nm (b,d) of HPTS dissolved in the solvents [D_6]DMSO (a,b) and D_2O (c,d).*

these initially highly populated Raman-active modes.[55–57] Subsequently the excess energy in the Raman-active modes is redistributed over all vibrational modes by internal vibrational energy redistribution (IVR), expected to occur on sub-picosecond time scales for molecules as large as HPTS, establishing eventually a Boltzmann population distribution of the vibrational modes. This still holds when a level crossing occurs on a time scale shorter than 100 fs.[56] Additionally the molecules show vibrational cooling due to coupling to the nearby solvent molecules, that typically occurs on a time scale of 5–20 ps.[56,57] The IR-active bands then blue-shift to the frequency position

that corresponds to the S_1 state without vibrational excess energy, as recorded for an excitation wavelength of 400 nm. Based on the limited excess energy and the fact that the investigated IR-active bands only show an initial red-shift, followed by a blue-shift without substantial changes in transient absorbance line shapes we are convinced that these IR-active bands in the 1500 cm^{-1} range remain in the $v=0$ state of the same electronic level throughout all pulse delays for excitation at 350 nm. This important observation does not support the nonadiabatic three-level LE-CT model for HPTS. According to the level structure of this model, excitation at 350 nm would predominantly promote the HPTS molecule to the Franck–Condon region of the S_2 (CT-^1L_a) state. The molecule will remain in this state, when solvent relaxation is faster than internal conversion to the S_1 (LE-^1L_b) state, and solvent relaxation leads to a stabilization of the S_2 (CT-^1L_a) state below the S_1 (LE-^1L_b) state. Otherwise, the molecule would first display internal conversion to its S_1 (LE-^1L_b) state, and subsequently has to convert back to the solvent-stabilized S_2 (CT-^1L_a) state. As stated above, we do not observe any of these transitions between electronic states in times exceeding 150 fs. The model can only hold if the dynamics of level crossings and solvent relaxation occur in a few tens of femtoseconds, unobservable with our current time resolution.

These findings thus strongly point to the case of an absorption band between 320–430 nm due to an electronic transition to a single electronic state. It is worth mentioning that in an investigation of the solvatochromic properties of HPTS only one electronic state was used.[46] Moreover, in a combined experimental and theoretical study of MPTS also one electronic state was regarded.[58] Finally, excess energy that is released after an electronic level crossing appears to be of minor magnitude, since for both H_2O and DMSO solvents excitation of HPTS at 400 nm does not lead to major signatures in the transient spectra indicating spectral shifting due to IVR and subsequent cooling phenomena. This hints at an energy difference of less than 1000 cm^{-1} between the LE(^1L_b) and CT(^1L_a) states.

3.3. Solvent-Dependent Electronic States in Pyranine

We now discuss our findings in the context of the proposed models for photoacidity. By comparison of the transient IR results of MPTS and HPTS we demonstrate the occurrence of two distinct solvent dependent electronic state configurations. The choice of solvent determines which electronic state configuration dominates. Since the photobase form of HPTS appears with a time constant of 90 ps (250 ps) in H_2O (D_2O), the existence of two excited electronic states are related to the photoacid form of HPTS. These two distinct states are reached within our time resolution of 150 fs in the three solvents we have used in our study. Using our time-resolved IR spectra only we cannot determine whether the electronic excited states that we observe from 150 fs onwards are identical to the states initially reached by the absorption of a photon, or if a level crossing occurs in, for example, water within 150 fs.

In any case, from the observation of at least two distinct excited electronic states of the photoacid form of HPTS we can exclude the simple (solvent-independent) two-state model that has historically been proposed first. We can also exclude the assignment of the two electronic excited states for MPTS and HPTS as observed in the three solvents [D_6]DMSO, MeOD and D_2O to the levels proposed to play a role in the ESHT model. In this model a level crossing occurs between the optically excited $^1\pi\pi^*$ to a $^1\pi\sigma^*$ state where both an electron and a proton have been transferred to the solvent. Since we observe similar phenomena in MPTS and in HPTS, whereas clearly MPTS is not able to exhibit a net hydrogen transfer to the solvent, a $^1\pi\sigma^*$ state is not considered to play a role in the solvent-dependent electronic state change. We note however, that this conclusion does not exclude the involvement of a $^1\pi\sigma^*$ state in the final step, where the photoacid converts to the photobase while donating a proton (deuteron) to the solvent. This process occurs clearly with much longer time constants of 90 ps (250 ps) in H_2O (D_2O), and is not considered to play a role in the phenomena on (sub)picosecond time scales discussed here.

Based on these findings we cannot support but also not exclude a nonadiabatic electronic state change in MPTS and in HPTS photoacid, from LE(^1L_b) to CT(^1L_a) as proposed by Tran-Thi et al.[40,41] This change may indeed occur in water, but not on a time scale of 2 ps. The dynamics of the electronic excited states on the 2 ps time scale as found with UV-pump/Vis-probe spectroscopy are unlikely due to electronic state level crossing, but supposedly caused by solvation dynamics of the solvent. Although Tran-Thi et al. ascribed only a 300 fs time component to solvent reorganization, we argue that solvation dynamics of water, typically taking place on a multitude of time scales extending from a few tens of femtoseconds to several tens of picoseconds[59–63] is responsible for the reported 2 ps component as well. We remark here that the effects of solvation dynamics on the optical transitions of HPTS are not straightforward. We have undertaken a detailed analysis, to be published elsewhere, of the time dependence of the oscillator strength of the excited state of HPTS in terms of time-dependent overlap between the transient absorption and stimulated emission bands, that is controlled by solvent relaxation. This results in a gradual increase in the overlap of excited state absorption and stimulated emission bands and in a gradual decrease of apparent (integrated) absorption band, akin to the situation found in structurally related 8-hydroxpyrene-1,3,6-trisdimethylsulfonamide (HPTA).[64]

In contrast, we argue that if an electronic level change takes place in H_2O/D_2O, it should occur faster than with our time resolution, whereas this state inversion does not take place in [D_6]DMSO. It could be that in the case of MeOD we are in an intermediate regime, with significant probabilities to find MPTS and HPTS in either of these two electronic states. In case the three-state LE-CT model, with the LE(^1L_b)→CT(^1L_a), holds we thus probe the vibrational band pattern of MPTS and HPTS in the LE(^1L_b) state in [D_6]DMSO for pulse delays in the range between 0.15 ps–1 ns whereas the photoacid CT(^1L_a) state is detected in H_2O/D_2O, slowly changing into the conjugate photobase, in the same time range. One consequence of an ultrafast state change in HPTS and MPTS on a time scale much shorter

than 150 fs, however, is that the interstate couplings are expected to be considerable, on the order of several hundreds of wavenumbers. We thus feel that an electronic state description in terms of pure LE(^1L_b) and CT(^1L_a) configurations is less appropriate. In the next section we propose that the strongly mixed ^1L_b–^1L_a model as suggested by Knochenmuss et al.[9,38] is a better description for HPTS and MPTS.

3.4. Strongly Mixed ^1L_b–^1L_a Model

Originally proposed[9,38] to explain the spectra of 1-naphthol in small ammonia clusters where excited-state proton transfer from 1-naphthol was observed, this model describes the S_1 and S_2 states of 1-naphthol in ammonia as being made of ^1L_b and ^1L_a states that are strongly mixed with each other. This means that the original orthogonallity of the two L states found in the parent molecule naphthalene is lost by the combined action of the O–H substituent at the alpha position of the naphthalene ring and by strong-polar interactions with the solvent. The two close lying singlet states then strongly interact with each other and mix. The extent of level mixing generally depends on the relative oscillator strength of the two transitions, the energy gap between the unmixed levels and the magnitude of the matrix element that mixes them. In this model the initial photoexcited state (the LE state) evolves adiabatically on the S_1 surface without level crossing. This evolution is mainly of intramolecular vibrational redistribution character.

A similar situation may prevail in HPTS and MPTS because of, apart from the presence of the O–H group, the combined action of the three sulfonate groups that are located at the 1,3- and 6-positions of the pyrene moiety and their interactions with polar solvents. Turning to HPTS and MPTS in solution, one thus needs to include this additional ingredient in the modeling, namely the extent of the ^1L_b–^1L_a mixing caused by the solvent. The stronger the polar interactions with the solvent are, the more efficient is the ^1L_b–^1L_a mixing. Tran-Thi et al. have calculated that the oscillator strength of the ^1L_a transition of HPTS-like molecule in the gas phase is about eight times larger than the corresponding oscillator strength of the ^1L_b transition.[41] Thus, mixing the ^1L_b and ^1L_a states of HPTS should result in a S_0–S_1 transition of HPTS having increasingly more ^1L_a character as the mixing between the states becomes larger. Within the framework of this model, the locally excited S_1 state of HPTS will become more ^1L_a-like as the polar interactions of HPTS with the solvent increase. This means considerable changes in the structure of the absorption spectra of HPTS as a function of the solvent. The LE state of HPTS is likely to evolve further towards having ^1L_a character as the solvent relaxes around the excited-state configuration of the photoacid. This evolution is likely to be ultrafast, dominated by the inertial part of solvent relaxation that usually makes up the major fraction of the relaxation. Furthermore, we note that the transient response of the O–H group may also be involved in this adiabatic change in the electronic state configuration. Dynamics of hydrogen bond interactions induced by electronic excitation have been shown to occur on sub-100 fs time scales with vibrational spectroscopy of hydrogen-bonded complexes of coumarin 102[54,65–67] and with electronic spectroscopy of 8-hydroxpyrene-1,3,6-trisdimethylsulfonamide (HPTA),[64] and are below the time resolution of our current experiment.

The electronic structure of HPTS and MPTS is likely to be even more complex, with the two lower excited singlet states mixing not only with each other, but also with higher electronic levels including CT levels. In particular, HPTS is an example for a photoacid where charge transfer is considerably stabilized by intermolecular hydrogen-bonding interaction in a "push–pull" fashion: The sulfonate groups act on the "pull" side and this action is stabilized by proton-donating solvents, while at the O–H side hydrogen-bonding interactions with proton-accepting solvents help to "push" negative charge away from the hydrogen atom toward the pyrene ring. Amphoteric polar solvents such as water and methanol are thus expected to enhance the CT character of the S_1 state of HPTS not only by nonspecific polar interactions but also by the combined action of their hydrogen-bonding interactions with the photoacid.

In Figure 14 we have attempted to analyze the absorption spectra of HPTS by the sum of two Pekarian functions[68–70] that were found to be the minimum number needed to simulate the absorption spectra. A similar procedure was previously used to model the ^1L_b and ^1L_a transitions of 1- and 2-naphthols.[39] Interestingly, in aprotic DMSO (Figure 14b) the low-energy Pekarian already resembles more a transition to a ^1L_a than to a ^1L_b state as judged by the appearance of the vibronic features (spacing of about 1220 cm^{-1} and width at half maxi-

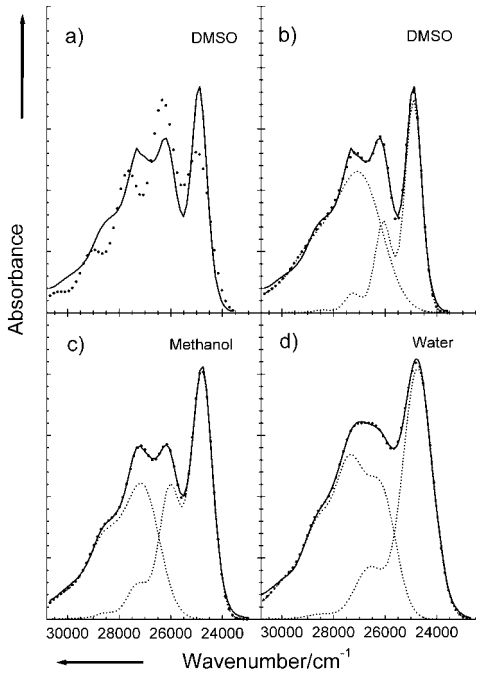

Figure 14. *Fit of the absorption spectra of HPTS in DMSO by one (a) and two (b) Pekarian functions, and in methanol (c) and in water (d) by two Pekarian functions. Experimental spectra are shown by solid lines. Calculated (best fit) Pekarian functions are indicated by full dots. The two components are depicted as dotted lines.*

mum of the first vibronic feature of about 700 cm^{-1}) in the absorption spectra.[71] The high-energy Pekarian appears featureless and consists of a much larger area than the low-frequency one. In H_2O the two Pekarians cover roughly the same area and seems to have changed toward a more common structure: The low-energy Pekarian becomes less structured while the high-energy Pekarian becomes more structured. Methanol (Figure 14c) seems to be a case in between the DMSO and H_2O extremes. The spectral analysis points to a solvent-dependent change in the shape of the absorption spectra of HPTS, as opposed to a simple overlap of two transitions with only their relative contributions to the overall absorption spectra being affected by the solvent. We conclude that the absorption spectrum of HPTS depends on the solvent in a complex way, confirming our main observations achieved with transient IR spectroscopy. Such complex solvent dependent level structure including vibronic changes is consistent with a level mixing scheme when one of the levels has CT properties.[72]

Summing-up, according to the ^1L_b–^1L_a mixing model, excitation of HPTS and MPTS in polar solvents occurs to an LE state being already of mixed ^1L_b–^1L_a character. The extent of mixing also depends on the strength of the polar interactions with the solvent. One thus expects changes in both the absorption and fluorescence spectra of HPTS due to specific (mainly hydrogen bonding) and unspecific polar interactions with the solvent. Transient changes in the spectra are then expected to be caused by solvent relaxation around the LE state, but these transient changes are likely to be on the time scale of the inertial response of the solvent and do not involve level crossing. In water and methanol solvents this means transients on the sub-100 fs time scale, which can not be resolved with our experimental time resolution. The optical properties of the S_1 state, as judged by the structure and location of the electronic spectra of the S_1 state, are expected to change considerably and rather continuously as a function of solvent polarity. This seems a fair description of the optical spectra of HPTS that have been gathered to date in various solvents, including the optical spectra of HPTS that we have analyzed herein.

4. Conclusions

We have used femtosecond mid-infrared spectroscopy to follow the dynamics of IR-active vibrational band patterns of the photoacid pyranine (HPTS) in liquid solutions. We have investigated the methoxy derivative of pyranine (MPTS) for comparison. Our results demonstrate that this method unequivocally shows that in the aprotic solvent dimethylsulfoxide an electronic state is reached, supposed to be of local excitation (LE) character according to theoretical considerations, without further dynamical changes of the fingerprint vibrations. The transient O–H stretching band indicates that HPTS forms a weak hydrogen bond with dimethylsulfoxide in the electronic excited state, that rearranges on (sub)picosecond time scales. In contrast, in the protic solvent water a different structure is reached after initial excitation of the LE state on a time scale faster than 150 fs, that likely has charge transfer (CT) character. We allocate a transient response between 2400–2850 cm^{-1} to be due to the O–H stretching oscillator of HPTS in H_2O, forming a medium-strong hydrogen bond with water. We assign the decay of this signal at (sub)picosecond time scales to be due to solvent rearrangement. We expect that more insight into the structure of the excited states of HPTS and MPTS can be obtained when the observed vibrational band patterns are connected to quantum-chemical calculations of these states. These may shed light on the exact nature of the large solvent effect on the structure of the first electronic excited state of HPTS including the question whether solvent-induced level switching or solvent induced level mixing are the acting mechanisms responsible for the solvent effect.

Acknowledgments

The progress has benefited from the financial support of the German–Israeli Foundation for Scientific Research and Development (Project GIF 722/01); B.Z.M. acknowledges financial travel support through the LIMANS Cluster of Large Scale Laser Facilities (Project MBI000228). O.F.M. is supported by a long term mission fellowship of the Egyptian government.

Keywords: hydrogen bonds · IR spectroscopy · photoacids · proton transfer · solvation

[1] T. Förster, *Naturwissenschaften* **1949**, *36*, 186.
[2] A. Weller, *Naturwissenschaften* **1955**, *42*, 175.
[3] A. Weller, *Progr. React. Kinet.* **1961**, *1*, 187.
[4] M. Eigen, *Angew. Chem.* **1964**, *76*, 1; *Angew. Chem. Int. Ed. Engl.* **1964**, *3*, 1.
[5] E. M. Kosower, D. Huppert, *Annu. Rev. Phys. Chem.* **1986**, *37*, 127.
[6] E. Pines, D. Pines in *Ultrafast hydrogen-bonding dynamics and proton transfer processes in the condensed phase, Vol.* 23 (Eds.: T. Elsaesser, H. J. Bakker), Kluwer Academic Publishers, Dordrecht, **2002**, pp. 155.
[7] L. M. Tolbert, K. M. Solntsev, *Acc. Chem. Res.* **2002**, *35*, 19
[8] J. Syage, *J. Phys. Chem.* **1995**, *99*, 5772.
[9] R. Knochenmuss, I. Fischer, *Int. J. Mass. Spectrom.* **2002**, *220*, 343.
[10] O. David, C. Dedonder-Lardeux, C. Jouvet, *Int. Rev. Phys. Chem.* **2002**, *21*, 499.
[11] E. Vander Donckt, *Progr. React. Kinet.* **1970**, *5*, 273.
[12] N. Mataga, T. Kubota, *Molecular Interactions and Electronic Spectra*, Marcel Dekker, New York, **1970**.
[13] L. G. Arnaut, S. J. Formosinho, *J. Photochem. Photobiol. A* **1993**, *75*, 1.
[14] M. Barroso, L. G. Arnaut, S. J. Formosinho, *J. Photochem. Photobiol. A* **2002**, *154*, 13.
[15] N. Agmon, W. Rettig, C. Groth, *J. Am. Chem. Soc.* **2002**, *124*, 1089.
[16] G. W. Robinson, P. J. Thistlethwaite, J. Lee, *J. Phys. Chem.* **1986**, *90*, 4224.
[17] J. Lee, G. W. Robinson, S. P. Webb, L. A. Philips, J. H. Clark, *J. Am. Chem. Soc.* **1986**, *108*, 6538.
[18] J. Lee, G. W. Robinson, M. P. Bassez, *J. Am. Chem. Soc.* **1986**, *108*, 7477.
[19] G. W. Robinson, *J. Phys. Chem.* **1991**, *95*, 10386.
[20] E. Pines, G. R. Fleming, *J. Phys. Chem.* **1991**, *95*, 10448.
[21] N. Agmon, D. Huppert, A. Masad, E. Pines, *J. Phys. Chem.* **1991**, *95*, 10407.
[22] E. Pines, B. Z. Magnes, M. J. Lang, G. R. Fleming, *Chem. Phys. Lett.* **1997**, *281*, 413.
[23] I. Carmeli, D. Huppert, L. M. Tolbert, J. E. Haubrich, *Chem. Phys. Lett.* **1996**, *260*, 109.
[24] E. Poles, B. Cohen, D. Huppert, *Isr. J. Chem.* **1999**, *39*, 347.
[25] B. Cohen, D. Huppert, *J. Phys. Chem. A* **2001**, *105*, 2980
[26] E. Pines, in *Chemistry of Phenols* (Ed.: Z. Rappoport), Wiley, New York, **2003**, pp. 491.

[27] J. W. Hager, D. R. Demmer, S. C. Wallace, *J. Phys. Chem.* **1987**, *91*, 1375.
[28] D. R. Demmer, G. W. Leach, E. A. Outhouse, J. W. Hager, S. C. Wallace, *J. Phys. Chem.* **1990**, *94*, 582.
[29] M. J. Tubergen, D. H. Levy, *J. Phys. Chem.* **1991**, *95*, 2175.
[30] S. Arnold, M. Sulkes, *J. Phys. Chem.* **1992**, *96*, 4768.
[31] D. R. Demmer, G. W. Leach, S. C. Wallace, *J. Phys. Chem.* **1994**, *98*, 12834.
[32] Y.-H. Huang, M. Sulkes, *J. Phys. Chem.* **1996**, *100*, 16479.
[33] K. W. Short, P. R. Callis, *J. Chem. Phys.* **2000**, *113*, 5235.
[34] P. R. Callis, *Methods Enzymol.* **1997**, *278*, 113.
[35] M. Raytchev, E. Pandurski, I. Buchvarov, C. Modrakowski, T. Fiebig, *J. Phys. Chem. A* **2003**, *107*, 4592.
[36] R. Knochenmuss, S. Leutwyler, *J. Chem. Phys.* **1989**, *91*, 1268.
[37] R. Knochenmuss, P. L. Muino, C. Wickleder, *J. Phys. Chem.* **1996**, *100*, 11218.
[38] R. Knochenmuss, I. Fischer, D. Lührs, Q. Lin, *Isr. J. Chem.* **1999**, *39*, 221.
[39] B.-Z. Magnes, N. V. Strashnikova, E. Pines, *Isr. J. Chem.* **1999**, *39*, 361.
[40] T. H. Tran-Thi, T. Gustavsson, C. Prayer, S. Pommeret, J. T. Hynes, *Chem. Phys. Lett.* **2000**, *329*, 421.
[41] T.-H. Tran-Thi, C. Prayer, P. Millié, P. Uznanski, J. T. Hynes, *J. Phys. Chem. A* **2002**, *106*, 2244
[42] J. T. Hynes, T. H. Tran-Thi, G. Granucci, *J. Photochem. Photobiol. A* **2002**, *154*, 3.
[43] A. L. Sobolewski, W. Domcke, C. Dedonder-Lardeux, C. Jouvet, *Phys. Chem. Chem. Phys.* **2002**, *4*, 1093.
[44] W. Domcke, A. L. Sobolewski, *Science* **2003**, *302*, 1693.
[45] C. Tanner, C. Manca, S. Leutwyler, *Science* **2003**, *302*, 1736.
[46] N. Barrash-Shiftan, B. B. Brauer, E. Pines, *J. Phys. Org. Chem.* **1998**, *11*, 743.
[47] A. Kummrow, M. Wittmann, F. Tschirschwitz, G. Korn, E. T. J. Nibbering, *Appl. Phys. B* **2000**, *B71*, 885.
[48] R. A. Kaindl, M. Wurm, K. Reimann, P. Hamm, A. M. Weiner, M. Woerner, *J. Opt. Soc. Am. B* **2000**, *17*, 2086.
[49] Gaussian 98 (Revision A.7), M. J. Frisch, G. W. Trucks, H. B. Schlegel, G. E. Scuseria, M. A. Robb, J. R. Cheeseman, V. G. Zakrzewski, J. A. Montgomery, R. E. Stratmann, J. C. Burant, S. Dapprich, J. M. Millam, A. D. Daniels, K. N. Kudin, M. C. Strain, O. Farkas, J. Tomasi, V. Barone, M. Cossi, R. Cammi, B. Mennucci, C. Pomelli, C. Adamo, S. Clifford, J. Ochterski, G. A. Petersson, P. Y. Ayala, Q. Cui, K. Morokuma, D. K. Malick, A. D. Rabuck, K. Raghavachari, J. B. Foresman, J. Cioslowski, J. V. Ortiz, B. B. Stefanov, G. Liu, A. Liashenko, P. Piskorz, I. Komaromi, R. Gomperts, R. L. Martin, D. J. Fox, T. Keith, M. A. Al-Laham, C. Y. Peng, A. Nanayakkara, C. Gonzalez, M. Challacombe, P. M. W. Gill, B. G. Johnson, W. Chen, M. W. Wong, J. L. Andres, M. Head-Gordon, E. S. Replogle, J. A. Pople, Gaussian, Inc., Pittsburgh, PA, **1998**.
[50] M. Rini, B.-Z. Magnes, E. Pines, E. T. J. Nibbering, *Science* **2003**, *301*, 349.
[51] M. Rini, D. Pines, B. Z. Magnes, E. Pines, E. T. J. Nibbering, *J. Chem. Phys.* **2004**, *121*, 9593.
[52] D. Hadži, S. Bratos, in *The Hydrogen Bond: Recent developments in theory and experiments, Vol.* II*: Structure and Spectroscopy* (Eds.: P. Schuster, G. Zundel, C. Sandorfy), North Holland, Amsterdam, **1976**, pp. 565.
[53] E. T. J. Nibbering, T. Elsaesser, *Chem. Rev.* **2004**, *104*, 1887
[54] C. Chudoba, E. T. J. Nibbering, T. Elsaesser, *J. Phys. Chem. A* **1999**, *103*, 5625.
[55] P. Hamm, S. M. Ohline, W. Zinth, *J. Chem. Phys.* **1997**, *106*, 519.
[56] M. Rini, A. Kummrow, J. Dreyer, E. T. J. Nibbering, T. Elsaesser, *Faraday Discuss.* **2002**, *122*, 79.
[57] M. Rini, J. Dreyer, E. T. J. Nibbering, T. Elsaesser, *Chem. Phys. Lett.* **2003**, *374*, 13.
[58] R. Jimenez, D. A. Case, F. E. Romesberg, *J. Phys. Chem. B* **2002**, *106*, 1090.
[59] R. Jimenez, G. R. Fleming, P. V. Kumar, M. Maroncelli, *Nature* **1994**, *369*, 471.
[60] R. M. Stratt, M. Maroncelli, *J. Phys. Chem.* **1996**, *100*, 12981.
[61] C. Rønne, P.-O. Åstrand, S. R. Keiding, *Phys. Rev. Lett.* **1999**, *82*, 2888.
[62] J. Stenger, D. Madsen, P. Hamm, E. T. J. Nibbering, T. Elsaesser, *Phys. Rev. Lett.* **2001**, *87*, 027401.
[63] J. Stenger, D. Madsen, P. Hamm, E. T. J. Nibbering, T. Elsaesser, *J. Phys. Chem. A* **2002**, *106*, 2341.
[64] E. Pines, D. Pines, Y.-Z. Ma, G. R. Fleming, *ChemPhysChem* **2004**, *5*, 1315.
[65] C. Chudoba, E. T. J. Nibbering, T. Elsaesser, *Phys. Rev. Lett.* **1998**, *81*, 3010.
[66] E. T. J. Nibbering, C. Chudoba, T. Elsaesser, *Isr. J. Chem.* **1999**, *39*, 333.
[67] D. K. Palit, T. Q. Zhang, S. Kumazaki, K. Yoshihara, *J. Phys. Chem. A* **2003**, *107*, 10798.
[68] J. J. Markham, *Rev. Mod. Phys.* **1959**, *31*, 956.
[69] V. Seshadri, V. M. Kenkre, *Phys. Rev. A* **1978**, *17*, 223.
[70] M. Pope, C. E. Swenberg, in *Electronic Processes in Organic Crystals*, Clarendon, Oxford, **1982**, pp. 15.
[71] I. B. Berlman, *Handbook of Fluorescence Spectra of Aromatic Molecules*, Academic Press, London, **1971**.
[72] A. M. Moran, A. Myers Kelley, S. Tretiak, *Chem. Phys. Lett.* **2003**, *367*, 293.

Received: October 25, 2004
Revised: January 27, 2005
Published online on March 14, 2005

